

See discussions, stats, and author profiles for this publication at: <https://www.researchgate.net/publication/229077089>

# Ab Initio Study of the Oxidation Reaction of CO by ClO Radicals

ARTICLE *in* THE JOURNAL OF PHYSICAL CHEMISTRY A · AUGUST 2003

Impact Factor: 2.69 · DOI: 10.1021/jp0348272

---

CITATIONS

6

---

READS

18

3 AUTHORS, INCLUDING:



**Florent Louis**

Université des Sciences et Technologies de Li...

45 PUBLICATIONS 398 CITATIONS

SEE PROFILE



**Carlos Gonzalez**

National Institute of Standards and Technolo...

111 PUBLICATIONS 12,585 CITATIONS

SEE PROFILE

## Ab Initio Study of the Oxidation Reaction of CO by ClO Radicals

Florent Louis,<sup>\*,†</sup> Carlos A. Gonzalez,<sup>\*,‡</sup> and Jean-Pierre Sawerysyn<sup>†</sup>

Physico-Chimie des Processus de Combustion et de l'Atmosphère (PC2A) UMR CNRS 8522, FR CNRS 2416 Centre d'Etudes et de Recherche Lasers et Applications (CERLA), Université des Sciences et Technologies de Lille, 59655 Villeneuve d'Ascq Cedex, France, and Computational Chemistry Group, Physical and Chemical Properties Division, National Institute of Standards and Technology, Gaithersburg, Maryland 20899

Received: March 31, 2003; In Final Form: August 14, 2003

The oxidation of carbon monoxide by ClO radicals was studied by ab initio molecular orbital theory calculations. Geometry optimizations and vibrational frequencies were computed using two methods: Møller–Plesset second-order perturbation theory (MP2), and quadratic configuration interaction in the space of single and double excitations (QCISD). Single-point energy calculations were performed at the QCISD level with triple excitations treated perturbatively (QCISD(T)) and the aug-cc-pVTZ basis set. Canonical transition state theory was used to predict the rate constants as a function of temperature (550–2500 K), and three-parameter Arrhenius expressions were obtained by fitting to the computed rate constants. The possible impact of the title reaction in combustion chemistry is also discussed.

## Introduction

To model the high-temperature oxidation processes occurring in the incineration of chlorinated hazardous wastes, kinetic data concerning the reactivity of chlorooxy radicals with major species such as carbon monoxide are needed. A recent study<sup>1</sup> of the ignition and combustion of ammonium perchlorate in a hydrogen atmosphere showed that ClO radicals are generated at 1400 K near the surface of the burner at the same level of concentration as the OH radicals. To the best of our knowledge, this is the first time that ClO radicals have been detected in flames including chlorinated compounds. Studies<sup>2</sup> of the equilibrium product distributions associated with the combustion of CH<sub>3</sub>Cl, CH<sub>2</sub>Cl<sub>2</sub>, and CHCl<sub>3</sub> in air show that the mole fractions of ClO radicals under fuel lean conditions (equivalence ratio  $\varphi$  = 0.5) are at least 100 as high as the ones of OH radicals at temperatures lower than 900 K and remain predominant until about 1100, 1500, and 1800 K for CH<sub>3</sub>Cl, CH<sub>2</sub>Cl<sub>2</sub>, and CHCl<sub>3</sub>, respectively. These estimates suggest that ClO might contribute to the oxidation of CO to CO<sub>2</sub> in the combustion of chlorinated hydrocarbons under air excess conditions. This contribution is expected to be largely predominant in oxidation processes of chlorinated organic species without hydrogen atoms. Very few determinations of the rate constant of the reaction ClO + CO → Cl + CO<sub>2</sub> have been published in the literature. Clyne and Watson<sup>3</sup> reported an upper limit to the rate constant at 587 K ( $k < 2.0 \times 10^{-15}$  cm<sup>3</sup>·molecule<sup>-1</sup>·s<sup>-1</sup>) for the reaction between ClO and CO. On the basis of these data, DeMore et al.<sup>4</sup> have estimated the following rate expression over the atmospheric temperature range (200–300 K):

$$k = 1.0 \times 10^{-12} \text{ (cm}^3 \cdot \text{molecule}^{-1} \cdot \text{s}^{-1}) \times \exp(-30764 \text{ (J} \cdot \text{mol}^{-1})/RT) \quad (1)$$

where the activation energy is assumed to be a lower limit.

To assess the relevance of the title reaction in the incineration of chlorinated hazardous waste, it is important to understand the mechanisms and kinetics of this reaction at combustion temperatures. High-level ab initio molecular orbital theory can be very helpful in the prediction of the kinetic parameters over a wide temperature range and in the understanding of the details of the mechanism governing the reaction ClO + CO → Cl + CO<sub>2</sub>. In this work, we apply this methodology combined with canonical transition state theory, to study the temperature dependence of the kinetics of this reaction. To our knowledge, this is the first theoretical study of the reaction between ClO and CO.

Computational Methods<sup>5</sup>

All calculations described were carried out with the Gaussian 98<sup>6</sup> suite of programs on a 4-processor Compaq, 32-processor NEC SX-5, and 32-processor Silicon Graphics Origin 2000 parallel computers. Fully optimized geometries, harmonic vibrational frequencies, and zero-point energy corrections (ZPE) of reactants, transition states, molecular complexes and products, were calculated with the unrestricted second-order Møller–Plesset perturbation theory (UMP2)<sup>7</sup> using the 6-311G(d) basis set.<sup>8</sup> Electron correlation was computed with second-order Møller–Plesset perturbation theory with full annihilation of spin contamination<sup>9</sup> as implemented in the Gaussian 98 package (noted PMP2 in our results). To confirm the connection of the transition states with reactants and products, the reaction path was followed using IRC<sup>10</sup> (intrinsic reaction coordinate) calculations at the UMP2/6-311G(d) level. The geometrical parameters were reoptimized with the unrestricted quadratic configuration interaction theory using single and double excitations method<sup>11</sup> (UQCISD) and the 6-311G(d) basis set. Harmonic vibrational frequencies were also computed numerically at the UQCISD/6-311G(d) level. The geometries previously optimized at the QCISD/6-311G(d) level were used in order to perform single-point energy calculations for all species at the quadratic configuration interaction level of theory using single, double, and triple excitations, QCISD(T),<sup>11</sup> and basis sets ranging from

\* To whom correspondence should be addressed. F.L.: fax, (33)-3-20436977; e-mail, florent.louis@univ-lille1.fr. C.G.: fax, (301)869-4020; e-mail, carlos.gonzalez@nist.gov.

<sup>†</sup> Université des Sciences et Technologies de Lille.

<sup>‡</sup> National Institute of Standards and Technology.

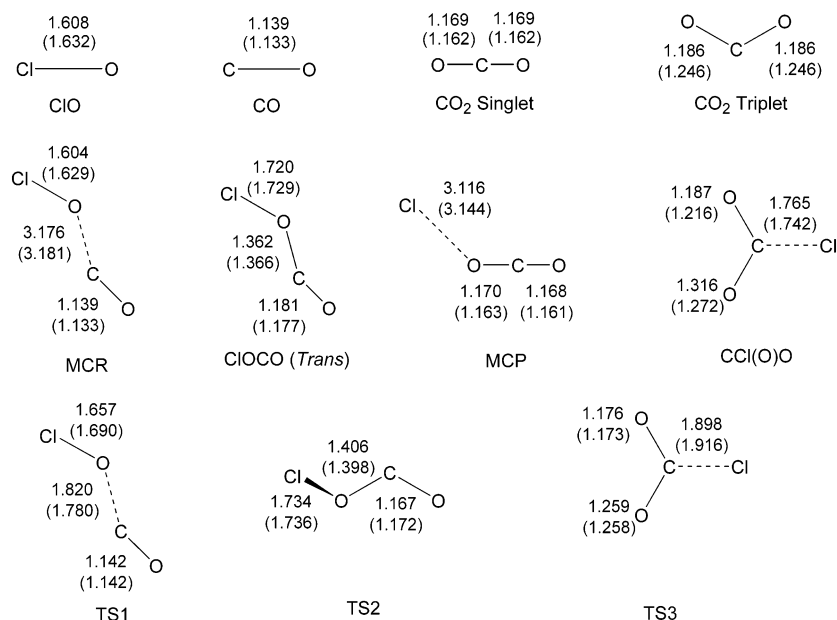


**Figure 1.** Structures optimized at UMP2/6-311G(d) and QCISD/6-311G(d) levels of theory for the reactants, products, and intermediate species. Bond lengths are in Ångströms. The values in parentheses correspond to the QCISD/6-311G(d) calculations.

**TABLE 1: Optimized Geometry Parameters<sup>a</sup> for Intermediate Species Calculated at UMP2/6-311G(d) and UQCISD/6-311G(d) Levels of Theory**

| parameter                       | MCR           | TS1           | ClOCO (trans) | TS2           | MCP           | TS3           | CCl(O)O       |
|---------------------------------|---------------|---------------|---------------|---------------|---------------|---------------|---------------|
| $r(\text{C}-\text{O}_1)$        | 1.139 (1.133) | 1.142 (1.142) | 1.181 (1.177) | 1.167 (1.172) | 1.168 (1.161) | 1.176 (1.173) | 1.187 (1.216) |
| $r(\text{C}-\text{O}_2)$        | 3.176 (3.181) | 1.820 (1.780) | 1.362 (1.366) | 1.406 (1.398) | 1.170 (1.163) | 1.259 (1.258) | 1.316 (1.272) |
| $r(\text{Cl}-\text{O}_2)$       | 1.604 (1.629) | 1.657 (1.690) | 1.720 (1.729) | 1.734 (1.736) | 3.116 (3.144) |               |               |
| $r(\text{C}-\text{Cl})$         |               |               |               |               |               | 1.898 (1.917) | 1.765 (1.742) |
| $\theta(\text{O}_2\text{CO}_1)$ | 102.0 (104.9) | 120.9 (120.0) | 124.2 (124.2) | 128.8 (128.4) | 179.9 (179.9) | 143.1 (142.9) | 128.1 (121.5) |
| $\theta(\text{ClO}_2\text{C})$  | 94.7 (94.9)   | 114.9 (113.9) | 112.0 (112.0) | 109.2 (110.1) | 136.8 (136.9) |               |               |
| $\theta(\text{ClCO}_1)$         |               |               |               |               |               | 124.3 (122.8) | 126.6 (123.0) |
| $\phi(\text{ClO}_2\text{CO}_1)$ | 188.9 (182.8) | 180.0 (180.0) | 180.0 (180.0) | 94.8 (97.4)   | 180.3 (179.9) |               |               |
| $\phi(\text{ClCO}_1\text{O}_2)$ |               |               |               |               |               | 180.0 (180.0) | 180.0 (180.0) |

<sup>a</sup> Bond lengths in Ångströms, angles in degrees; values in parentheses correspond to the optimized geometries at the UQCISD/6-311G(d) level.

**TABLE 2: Vibrational Frequencies and Zero-Point Energy (ZPE) Corrections for Intermediate Species Calculated at UMP2/6-311G(d) and UQCISD/6-311G(d) Levels of Theory**

| species       | vibrational frequencies ( $\text{cm}^{-1}$ ) <sup>a</sup>                          | ZPE ( $\text{kJ}\cdot\text{mol}^{-1}$ ) |
|---------------|--|---|
| MCR           | 9, 48, 53, 102, 828, 2137<br>8, 50, 53, 105, 776, 2190                             | 19.0<br>19.0                            |
| TS1           | <b>671i</b> , 95, 202, 328, 865, 2095<br><b>604i</b> , 107, 209, 357, 727, 2082    | 21.4<br>20.8                            |
| ClOCO (trans) | 219, 286, 530, 893, 1055, 1886<br>206, 282, 498, 792, 1033, 1897                   | 29.1<br>28.2                            |
| TS2           | <b>295i</b> , 234, 584, 704, 885, 2127<br><b>291i</b> , 245, 573, 699, 876, 1893   | 27.1<br>25.6                            |
| MCP           | 14, 59, 656, 657, 1342, 2456<br>12, 56, 673, 674, 1375, 2431                       | 31.0<br>31.3                            |
| TS3           | <b>727i</b> , 415, 429, 660, 1058, 2027<br><b>555i</b> , 383, 444, 661, 1104, 2014 | 27.4<br>27.5                            |
| CCl(O)O       | 321, 462, 670, 674, 1127, 1878<br>330, 458, 665, 697, 1168, 1478                   | 30.7<br>28.7                            |

<sup>a</sup> First row represents UMP2/6-311G(d) calculations, and second row, UQCISD/6-311G(d) calculations.

6-311G(d) to the augmented correlation-consistent polarized valence triple- $\zeta$  sets,<sup>12</sup> aug-cc-pVTZ, developed by Kendall et al.

## Results and Discussion

The structures of all stationary points involved in this reaction are shown in Figure 1. Tables 1 and 2 list the corresponding optimized geometrical parameters, vibrational frequencies, and

unscaled zero-point energy corrections (ZPEs). Given that instabilities of the HF/3-21G wave function for the  $C_{2v}$  structure of the  $\text{ClCO}_2$  radical previously observed by Marshall<sup>13</sup> cast some doubts on the applicability of the single-reference treatments of potential energy surfaces involving chlorine and carbon monoxide, stability tests were conducted on the Hartree-Fock (HF) wave functions corresponding to all stationary points optimized in this study. The results show that for all the basis sets used in this work, these stationary points are characterized by stable HF wave functions, providing grounds for confidence on the validity of the single-reference based calculations performed in the present study.

**1. Reaction Mechanism and Energetics. 1.1. ClOC•O and CCl(O)O• Radicals.** Given that a concerted addition mechanism could lead to the formation of the  $\text{ClOC}\cdot\text{O}$  and the  $\text{CCl}(\text{O})\text{O}\cdot$  radicals, we decided to characterize the geometrical properties as well as the energetics of these species. The  $\text{ClOC}\cdot\text{O}$  radical can in principle be found in a trans and a cis conformer with the  $\text{Cl}-\text{O}-\text{C}-\text{O}$  dihedral angle  $\phi$  equal to  $180^\circ$  and  $0^\circ$ , respectively. The trans structure was optimized at both levels of theory (see Figure 1). Direct geometry optimizations at the MP2 and QCISD calculations predict a very unstable cis conformer that decomposes into the more stable system  $\text{Cl} + \text{CO}_2$  as a result of the cleavage of the  $\text{Cl}-\text{O}$  bond. Similar results were obtained at the UHF<sup>14</sup> and B3LYP<sup>15</sup> levels. To further investigate these results, the rotational potential energy surface (RPES) for the  $\text{ClOC}\cdot\text{O}$  radical was computed at the UMP2/

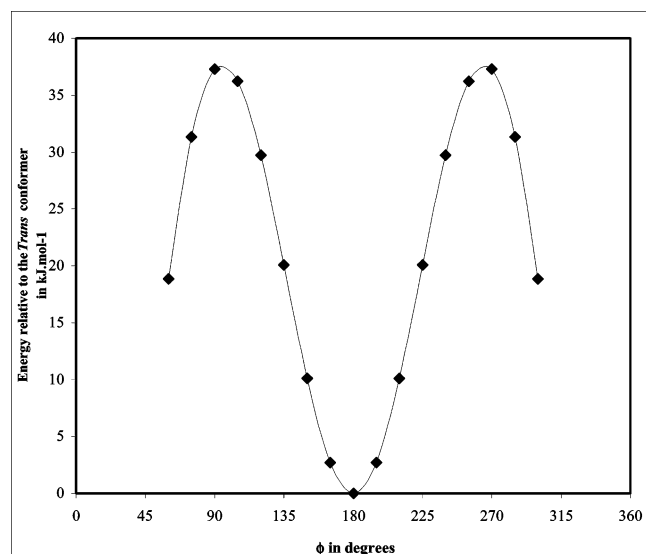


**Figure 2.** Rotational potential energy surface for the ClO•O radical calculated at the UMP2/6-311G(d) level of theory.

**TABLE 3: Energies of All Stationary Points Relative to ClO + CO Calculated at the QCISD(T)/aug-cc-pVTZ//QCISD/6-311G(d) Level of Theory Including the ΔZPEs**

| species                        | energy/ClO + CO in kJ·mol <sup>-1</sup> |
|--------------------------------|---|
| MCR                            | -3.0                                    |
| TS1                            | 48.9                                    |
| CIOCO (trans)                  | 1.1                                     |
| TS2                            | 29.9                                    |
| MCP                            | -271.2                                  |
| Cl + CO <sub>2</sub> (singlet) | -266.9                                  |
| Cl + CO <sub>2</sub> (triplet) | 163.9                                   |
| TS3                            | -162.1                                  |
| CCl(O)O                        | -160.9                                  |

6-311G(d) (see Figure 2). The RPES was obtained by performing a relaxed scan starting from the trans conformer ( $\phi = 180^\circ$ ) where  $\phi$  was varied by  $15^\circ$  intervals. As observed in Figure 2, the RPES is characterized by a rotational transition state that connects the trans conformer with a nonstationary point in the vicinity of  $60^\circ$ . The dihedral angle for the corresponding transition structure was found to be equal to  $94.8^\circ$  at the UMP2/6-311G(d) level of theory. This structure is indeed a first-order saddle point with an imaginary frequency of  $295i \text{ cm}^{-1}$ . In addition, it was found that for  $\phi$  values lower than  $60^\circ$ , the relaxed scan failed to locate a stationary point, suggesting the nonexistence of the cis conformer. Furthermore, IRC calculations indicate that the rotational transition state connects the trans conformer with a  $\text{Cl}\cdots\text{CO}_2$  molecular complex instead the cis conformer. From these results, we conclude that the *cis*-ClO•O radical does not exist.

Despite exhaustive searches involving relaxed scans and IRC calculations, we were not able to locate a pathway connecting the ClO•O and CCl(O)O• radicals, indicating that the isomerization reaction involving these radicals is unlikely. This is in agreement with the QCISD(T)/6-311G(2d) calculations of Su and Francisco<sup>16</sup> on the FO + CO reaction, where a fairly large intrinsic barrier ( $243.5 \text{ kJ}\cdot\text{mol}^{-1}$ ) for the isomerization *trans*-FO•O → CF(O)O•, was found.

**1.2. ClO + CO Reaction Pathway and Energetics.** Table 3 lists the relative energies (computed at QCISD(T)/aug-cc-pVTZ//QCISD/6-311G(d) level) of the different stationary points located along the ClO + CO reaction pathway, and Figure 3 depicts the corresponding energy profile. The first step of the addition of ClO radicals to carbon monoxide involves the

formation of a molecular complex (MCR in Figure 3), which lies approximately  $3.0 \text{ kJ mol}^{-1}$  below reactants. This complex is characterized by an intermolecular distance of  $3.2 \text{ \AA}$  and is the result of long-range interactions between CO and the ClO radical. MCR undergoes a structural rearrangement that leads to the formation of the *trans*-ClO•O radical, which lies approximately  $1.1 \text{ kJ mol}^{-1}$  above reactants. These two stationary points are connected by a transition structure (TS1 in Figure 3), characterized by an  $\text{OC}\cdots\text{OCl}$  bond length of about  $1.820 \text{ \AA}$ , which is significantly larger than the corresponding bond length in the *trans*-ClO•O intermediate ( $1.362 \text{ \AA}$ ). The intrinsic barrier for the  $\text{MCR} \rightarrow \text{trans-ClO}\cdot\text{O}$  step was computed to be  $52 \text{ kJ mol}^{-1}$ . The results of our calculations indicate that once formed, the *trans*-ClO•O radical undergoes a rotation around the  $\text{OCl-OC}$  bond that leads to a transition structure (TS2 in Figure 3)  $29.9 \text{ kJ mol}^{-1}$  higher than reactants with a dihedral angle  $\phi = 94.8^\circ$ . This transition structure leads to the formation of a molecular complex (MCP in Figure 3), which is approximately  $271.2 \text{ kJ mol}^{-1}$  more stable than reactants, and that decomposes to the products  $\text{Cl} + {}^1\text{CO}_2$ . As Figure 2 shows, this stationary point is mainly a  $\text{Cl}\cdots\text{CO}_2$  long-range complex, with a  $\text{Cl}\cdots\text{O}$  bond distance equal to  $3.1 \text{ \AA}$  (computed at the QCISD(T)/aug-cc-pVTZ//QCISD/6-311G(d) level). In addition, a transition state structure (TS3 in Figure 3), connecting the radical  $\text{CCl(O)O}\cdot$  and the more stable products  $\text{Cl} + {}^1\text{CO}_2$  was located at all levels of theory used in this work. After zero point energy corrections are taken into account, it is found that the TS3 energy lies below the energy of  $\text{CCl(O)O}\cdot$ , indicating that this radical readily dissociates into Cl and  ${}^1\text{CO}_2$ . Finally, the dissociation of the *trans*-ClO•O radical to Cl and  ${}^3\text{CO}_2$  was found to be significantly endothermic, casting some doubts over the relevance of this step in the studied temperature range.

The theoretical predicted value for the reaction enthalpy at 298 K for the oxidation reaction computed at the QCISD(T)/aug-cc-pVTZ//QCISD/6-311G(d) level of theory is  $-268.9 \text{ kJ mol}^{-1}$ , which is in good agreement with the corresponding literature value of  $-263.3 \pm 0.4 \text{ kJ mol}^{-1}$  on the basis of  $\Delta_f H^\circ$  at 298 K for ClO,<sup>17</sup> CO,<sup>18</sup> Cl,<sup>17</sup> and CO<sub>2</sub>.<sup>17</sup> This agreement justifies the use of the levels of theory employed in this work.

**2. Rate Constant Calculations.** Given the mechanism and energetics predicted by our calculations, it would seem reasonable to assume that the bottleneck of the reaction is determined by the entrance channel where the reactive system has to overcome a barrier of approximately  $49 \text{ kJ mol}^{-1}$  corresponding to the transition structure TS1. Canonical transition state theory<sup>19</sup> (TST) including a semiclassical one-dimensional multiplicative tunneling correction factor was used to predict the temperature dependence of the rate constant. The rate constants,  $k(T)$ , were computed using the following expression:

$$k(T) = \Gamma(T) \frac{k_B T}{h} \frac{Q_{\text{TS1}}(T)}{Q_{\text{ClO}}(T) Q_{\text{CO}}(T)} \exp\left(-\frac{E_0}{k_B T}\right) \quad (2)$$

where  $\Gamma(T)$  indicates the transmission coefficient used for the tunneling correction at temperature  $T$ ,  $Q_{\text{TS1}}(T)$ ,  $Q_{\text{ClO}}(T)$ , and  $Q_{\text{CO}}(T)$  are the total partition functions for the transition state TS1, ClO radical, and CO at temperature  $T$ ,  $E_0$  is the vibrationally adiabatic barrier height computed as the difference in energies between the transition state TS1 and reactants, including zero point energy corrections,  $k_B$  is Boltzmann's constant, and  $h$  is Planck's constant.

The multiplicity of the  ${}^2\Pi_{3/2}$  and  ${}^2\Pi_{1/2}$  states and the corresponding energy gap of  $320.3 \text{ cm}^{-1}$  for ClO between the low-lying electronic states<sup>18</sup> have been explicitly included in

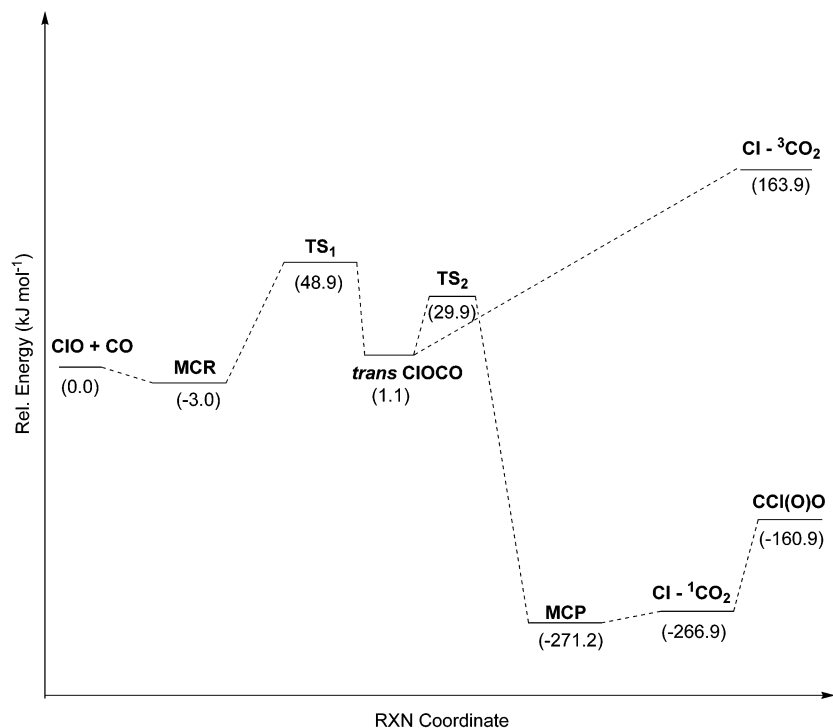


**Figure 3.** Schematic diagram of the potential energy surface profile for the ClO + CO reaction calculated at the QCISD(T)/aug-cc-pVTZ//QCISD/6-311G(d) level of theory.

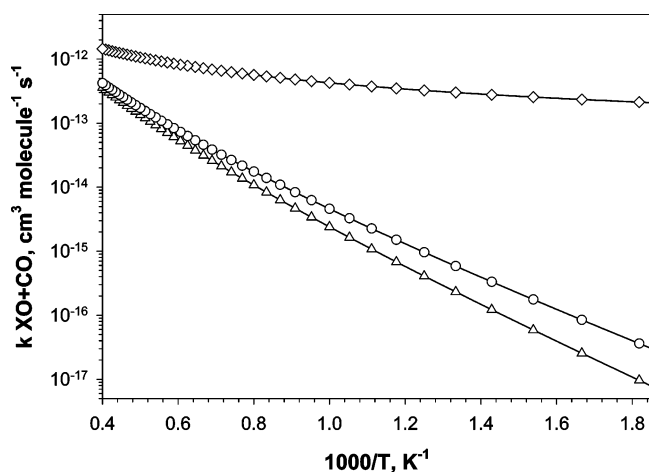


**Figure 4.** Temperature dependence of the rate constants for HO + CO (diamonds), FO + CO (circles), and ClO + CO (triangles).

the computation of the electronic partition function. All vibrations were treated as harmonic oscillators. We adopt the simple and computationally inexpensive Wigner method<sup>20</sup> in the estimation of the tunneling corrections for the reaction reported in this work:

$$\Gamma(T) = 1 + \frac{1}{24} \left( \frac{h\nu^\ddagger}{k_B T} \right)^2 \quad (3)$$

where  $\nu^\ddagger$  is the imaginary frequency at the saddle point. This choice seems to be appropriate for the treatment of tunneling corrections of rate constants calculated at typical incineration/combustion temperatures (550–2500 K) for which the values of transmission coefficient  $\Gamma(T)$  are close to 1 (e.g.,  $\Gamma(550 \text{ K}) = 1.10$ ). Rate constant calculations were carried out over the temperature range of interest using the Turbo-Opt program.<sup>21</sup>

Figure 4 depicts the computed Arrhenius plot in the temperature range 550–2500 K. The rate constants plotted in Figure

4 have been fitted to a three-parameter formula by least-squares, giving the following relation (in units of  $\text{cm}^3 \cdot \text{molecule}^{-1} \cdot \text{s}^{-1}$ ):

$$k(550\text{--}2500 \text{ K}) = (4.0 \times 10^{-19}) T^{2.02} e^{(-5265/T)} \quad (4)$$

It is interesting to note that using eq 4, a value  $k(587 \text{ K})$  calculated for the rate constant of the ClO + CO reaction is 2 orders of magnitude below the upper limit value proposed by Clyne and Watson<sup>3</sup> ( $2.0 \times 10^{-17} \text{ cm}^3 \text{ molecule}^{-1} \text{ s}^{-1}$  vs  $2.0 \times 10^{-15} \text{ cm}^3 \text{ molecule}^{-1} \text{ s}^{-1}$ ).

#### Comparison of the $\text{OX} + \text{CO} \rightarrow \text{X} + \text{CO}_2$ Reactions ( $\text{X} = \text{Cl}$ or $\text{F}$ ) to $\text{OH} + \text{CO} \rightarrow \text{H} + \text{CO}_2$

The reaction  $\text{OH} + \text{CO} \rightarrow \text{CO}_2 + \text{H}$  has been extensively studied experimentally and theoretically. The Arrhenius plot for this reaction is depicted in Figure 4. This plot is based on the parameters proposed by Baulch et al.<sup>22</sup> in their 1992 evaluation:

$$k(T) = 5.4 \times 10^{-14} (\text{cm}^3 \cdot \text{molecule}^{-1} \cdot \text{s}^{-1}) (T/298 \text{ K})^{1.50} e^{(250/T)} \quad (5)$$

The reaction of FO radicals with CO has been studied theoretically by Su and Francisco.<sup>16</sup> Similar to our results, they found that the addition of FO to CO is the rate-determining step in the complex mechanism. Because no rate constants were computed in their study, we re-optimized the geometries for reactants and the transition structure reported by these researchers using our methodology. Single-point energy calculations were performed at the QCISD(T)/aug-cc-pVTZ//QCISD/6-311G(d) level. Rate constants were calculated over the same temperature range as for the ClO + CO reaction and have been fitted to a three-parameter formula by the least-squares, giving the following relation (in units of  $\text{cm}^3 \cdot \text{molecule}^{-1} \cdot \text{s}^{-1}$ ):

$$k(550\text{--}2500 \text{ K}) = (3.2 \times 10^{-19}) T^{2.03} e^{(-4440/T)} \quad (6)$$



It is observed that over the same temperature range, the rate constants for the reaction  $\text{FO} + \text{CO}$  are close to the corresponding values for the reaction  $\text{ClO} + \text{CO}$  and substantially lower than the ones corresponding to the reaction  $\text{OH} + \text{CO}$ . The lack of experimental data on the ClO concentration profiles under incineration conditions does not enable us to directly compare the rate of  $\text{ClO} + \text{CO}$  reaction with the ones of  $\text{OH} + \text{CO}$  reaction, which is well-known to play an important role in the oxidation of CO. However, ClO and OH concentrations can be reasonably estimated from simulations of a detailed chemical mechanism, leading to a good agreement between the calculated and measured concentration profiles of molecular products generated by the oxidation processes. Numerical simulation of oxidation processes of some chlorinated hydrocarbons can help to better understand the relative importance of these two processes of oxidation of CO to  $\text{CO}_2$ . In our laboratory,<sup>23</sup> the processes of the thermal oxidation of 1300 ppm (v/v) of  $\text{CH}_2\text{Cl}_2$  in air were experimentally investigated at 1 atm over the temperature range 973–1173 K and residence times ranging from 0.5 to 3 s. A detailed chemical mechanism based on the model proposed by Bozzelli et al.<sup>24</sup> enabled us to assess the role played by radicals such as ClO and OH in the degradation processes of  $\text{CH}_2\text{Cl}_2$ , and in particular their respective role in the evolution of the CO concentration as a function of temperature and residence time. Analysis of reaction fluxes shows that the oxidation of CO to  $\text{CO}_2$  by ClO radicals is the dominant pathway at temperatures lower than 1000 K under our operating conditions (large air excess). The same results indicate that at higher temperatures, the oxidation of CO to  $\text{CO}_2$  by OH radicals becomes predominant. A similar analysis of elementary processes responsible for the conversion of CO to  $\text{CO}_2$  has also been performed<sup>25</sup> for the thermal oxidation of 1,3-hexachlorobutadiene (1,3- $\text{C}_4\text{Cl}_6$ ) under fuel lean conditions (1000 ppm v/v in 1 atm of air). In this case, the  $\text{CO} + \text{ClO} \rightarrow \text{CO}_2 + \text{Cl}$  reaction was found to be the most important pathway in the oxidation of CO into  $\text{CO}_2$  over the whole temperature range (compared to the two other possible CO oxidation processes:  $\text{CO} + \text{O}_2 \rightarrow \text{CO}_2 + \text{O}$  and  $\text{CO} + \text{O} + \text{M} \rightarrow \text{CO}_2 + \text{M}$ ). Therefore, our results show that although the rate constant of the  $\text{CO} + \text{ClO} \rightarrow \text{CO}_2 + \text{Cl}$  reaction is consistently lower than the one of the  $\text{CO} + \text{OH} \rightarrow \text{CO}_2 + \text{H}$  reaction over a wide temperature range ( $k_{\text{CO}+\text{OH}}/k_{\text{CO}+\text{ClO}} \sim 200$  at 1000 K and  $k_{\text{CO}+\text{OH}}/k_{\text{CO}+\text{ClO}} \sim 3.75$  at 2500 K), the relative importance of these two processes in the oxidation of CO also depends on the concentrations of ClO and OH radicals generated under operating conditions. Excess air (fuel lean conditions), low temperatures and a low content of H atoms in the chemical composition of the chlorinated species favor the oxidation of CO to  $\text{CO}_2$  by ClO radicals in their thermal processes of oxidative degradation. Our results suggest the need for direct measurements of ClO radicals under combustion conditions in order to assess the importance of the ClO radicals in the  $\text{CO} \rightarrow \text{CO}_2$  oxidation process.

## Conclusion

Ab initio electronic structure calculations, combined with canonical transition state theory, carried out on the oxidation reaction of CO by ClO radicals, lead to the conclusion that the addition of ClO to CO is the rate-determining step, characterized by lower rate constants than those obtained for the reaction of  $\text{OH} + \text{CO} \rightarrow \text{H} + \text{CO}_2$ . The relative importance of these reaction pathways to convert CO into  $\text{CO}_2$  in the thermal degradation processes of chlorinated species depends on the concentration of ClO and OH radicals generated under the

operating conditions. Our results indicate that despite the relative low rate constants for the  $\text{ClO} + \text{CO}$  reaction (as compared to  $\text{CO} + \text{OH}$ ), this reaction becomes the dominant pathway in the oxidation of CO in combustion processes characterized by excess air, relatively low temperatures and a low content of hydrogen atoms in the chemical composition of the chlorinated species involved in the combustion process.

**Acknowledgment.** We thank the CERLA and the “Institut du Développement et des Ressources en Informatique Scientifique” (IDRIS) for providing computing time for part of the theoretical calculations respectively under projects MUST and 20042. We are also grateful to the “Ministère de la Recherche et de l’Enseignement Supérieur”, the “Région Nord/Pas de Calais”, and the “Fonds Européen de Développement Economique des Régions” (FEDER) for partial funding of this work and for supporting CERLA. We also thank Pr. Joseph W. Bozzelli (New Jersey Institute of Technology) for fruitful discussions.

## References and Notes

- (1) Yuasa, S.; Yushina, S.; Uchida, T.; Shiraishi, N. *Proc. Combust. Inst.* **2000**, 28, 863.
- (2) Senkan, S. M. *Pollutants from Combustion. Formation and Impact on Atmospheric Chemistry*; Vovelle, C., Ed.; NATO Sciences Series, Series C; Kluwer Academic Press: Dordrecht, The Netherlands, 2000; p 547.
- (3) Clyne, M. A. A.; Watson, R. T. *J. Chem. Soc., Faraday Trans. 1* **1974**, 70, 2250.
- (4) DeMore, W. B.; Sander, S. P.; Golden, D. M.; Hampson, R. F.; Kurylo, M. J.; Howard, C. J.; Ravishankara, A. R.; Kolb, C. E.; Molina, M. J. *JPL Publication 97-4* **1997**, Evaluation 12.
- (5) The identification of commercial equipment or materials does not imply recognition or endorsement by the National Institute of Standards and Technology nor does it imply that the material or equipment identified are necessarily the best available for the purpose.
- (6) Frisch, M. J.; Trucks, G. W.; Schlegel, H. B.; Scuseria, G. E.; Robb, M. A.; Cheeseman, J. R.; Zakrzewski, V. G.; Montgomery, J. A., Jr.; Stratmann, R. E.; Burant, J. C.; Dapprich, S.; Millam, J. M.; Daniels, A. D.; Kudin, K. N.; Strain, M. C.; Farkas, O.; Tomasi, J.; Barone, V.; Cossi, M.; Cammi, R.; Mennucci, B.; Pomelli, C.; Adamo, C.; Clifford, S.; Ochterski, J.; Petersson, G. A.; Ayala, P. Y.; Cui, Q.; Morokuma, K.; Malick, D. K.; Rabuck, A. D.; Raghavachari, K.; Foresman, J. B.; Cioslowski, J.; Ortiz, J. V.; Baboul, A. G.; Stefanov, B. B.; Liu, G.; Liashenko, A.; Piskorz, P.; Komaromi, I.; Gomperts, R.; Martin, R. L.; Fox, D. J.; Keith, T.; Al-Laham, M. A.; Peng, C. Y.; Nanayakkara, A.; Gonzalez, C.; Challacombe, M.; Gill, P. M. W.; Johnson, B.; Chen, W.; Wong, M. W.; Andres, J. L.; Gonzalez, C.; Head-Gordon, M.; Replogle, E. S.; Pople, J. A. *Gaussian 98*, revision A.7; Gaussian, Inc.: Pittsburgh, PA, 1998.
- (7) Möller, C.; Plesset, M. S. *Phys. Rev.* **1934**, 46, 618.
- (8) Descriptions of the Pople-style basis sets can be found in the following: Foresman, J. B.; Frisch, A. E. *Exploring Chemistry with Electronic Structure Methods*, 2nd ed.; Gaussian, Inc.: Pittsburgh, PA, 1996.
- (9) (a) Schlegel, H. B. *J. Chem. Phys.* **1986**, 84, 4530. (b) Schlegel, H. B. *J. Phys. Chem.* **1988**, 92, 3075 (c) Sosa, C.; Schlegel, H. B. *Int. J. Quantum Chem.* **1986**, 29, 1001. (d) Sosa, C.; Schlegel, H. B. *Int. J. Quantum Chem.* **1987**, 30, 155.
- (10) Gonzalez, C.; Schlegel, H. B. *J. Chem. Phys.* **1989**, 90, 2154.
- (11) Pople, J. A.; Head-Gordon, M.; Raghavachari, K. *J. Chem. Phys.* **1987**, 87, 5968.
- (12) Kendall, R. A.; Dunning, T. H., Jr.; Harrison, R. J. *J. Chem. Phys.* **1992**, 96, 6796.
- (13) Marshall, P. J. *Mol. Struct. (THEOCHEM)* **1991**, 236, 309.
- (14) (a) Hartree, D. R. *Proc. Cambridge Philos. Soc.* **1928**, 24, 89. (b) Fock, V. Z. *Phys.* **1930**, 61, 126. (c) Slater, J. C. *Phys. Rev.* **1930**, 35, 210.
- (15) Becke, A. D. *J. Chem. Phys.* **1993**, 98, 5648.
- (16) Su, Y.; Francisco, J. S. *J. Phys. Chem. A* **1997**, 101, 1172.
- (17) Cox, J. D.; Wagman, D. D.; Medvedev, V. A. *CODATA Key Values for Thermodynamics*; Hemisphere Publishing Corp.: New York, 1989.
- (18) Chase, M. W. NIST-JANAF Thermochemical Tables. *J. Phys. Chem. Ref. Data Monograph* 9, 1998.
- (19) (a) Johnston, H. S. *Gas-Phase Reaction Rate Theory*; The Roland Press Co.: New York, 1966. (b) Laidler, K. J. *Theories of Chemical Reaction Rates*; McGraw-Hill: New York, 1969. (c) Weston, R. E.; Schwartz, H. A. *Chemical Kinetics*; Prentice Hall: New York, 1972. (d)

Rapp, D. *Statistical Mechanics*; Holt, Reinhard, and Winston: New York, 1972. (e) Nikitin, E. E. *Theory of Elementary Atomic and Molecular Processes in Gases*; Clarendon Press: Oxford, 1974. (f) Smith, I. W. M. *Kinetics and Dynamics of Elementary Gas Reactions*; Butterworth: London, 1980. (g) Steinfeld, J. I.; Francisco, J. S.; Hase, W. L. *Chemical Kinetics and Dynamics*; Prentice Hall: Englewood Cliffs, NJ, 1989.

(20) Wigner, E. P. *Z. Phys. Chem.* **1932**, B19, 203.

(21) Rate constants calculated with the Turbo-Rate module in the beta version of the TURBO-OPT geometry optimization package, developed by C. Gonzalez and T. Allison, National Institute of Standards and Technology, Gaithersburg, MD.

(22) Baulch, D. L.; Cobos, C. J.; Cox, R. A.; Esser, C.; Frank, P.; Just, Th.; Kerr, J. A.; Pilling, M. J.; Troe, J.; Walker, R. W.; Warnatz, J. *J. Phys. Chem. Ref. Data* **1992**, 21, 411.

(23) Fadli, A.; Baillet, C.; Bozzelli J. W.; Sawerysyn J.-P. To be published.

(24) (a) Ho W.-P.; Barat R. B.; Bozzelli J. W. *Combust. Flame* **1992**, 88, 265. (b) Ho W.-P.; Bozzelli J. W. *24th International Symposium on Combustion*; The Combustion Institute: Pittsburgh, PA, 1992; pp 743–748.

(25) Zhu, L.; Baillet, C.; Sawerysyn, J.-P.; Bozzelli, J. W. To be published.